In press
Journal of Neurophysiology
August, 2013

Loss of balance during balance beam walking elicits a multi-focal theta band electrocortical response

Amy R. Sipp[1]*, Joseph T. Gwin[1], Scott Makeig[2], Daniel P. Ferris[1]

[1] Human Neuromechanics Laboratory, University of Michigan, Ann Arbor, MI
[2] Swartz Center for Computational Neuroscience, University of California, San Diego, CA

* Corresponding Author:

Amy Sipp
School of Kinesiology
401 Washtenaw Ave.
Ann Arbor, MI, 48109
amysipp@umich.edu
phone: 734-647-5514
fax: 734-936-1925

Abstract

Determining the neural correlates of loss of balance during walking could lead to improved clinical assessment and treatment for individuals predisposed to falls. We used high-density electroencephalography (EEG) combined with independent component analysis (ICA) to study loss of balance during human walking. We examined 26 healthy young subjects performing heel-to-toe walking on a treadmill-mounted balance beam as well as walking on the treadmill belt (both at 0.22 m/s). ICA identified clusters of electrocortical EEG sources located in or near anterior cingulate, anterior parietal, superior dorsolateral prefrontal and medial sensorimotor cortex that exhibited significantly larger mean spectral power in the theta band (4-7 Hz) during walking on the balance beam compared to treadmill walking. Left and right sensorimotor cortex clusters produced significantly less power in the beta band (12-30 Hz) during walking on the balance beam compared to treadmill walking. For each source cluster, we also computed a normalized mean time/frequency spectrogram time locked to the gait cycle during loss of balance (i.e., when subjects stepped off the balance beam). All clusters except the medial sensorimotor cluster exhibited a transient increase in theta band power during loss of balance. Cluster spectrograms demonstrated that the first electrocortical indication of impending loss of balance occurred in the left sensorimotor cortex at the transition from single support to double support prior to stepping off the beam. These findings provide new insight into the neural correlates of walking balance control and could aid future studies on elderly individuals and others with balance impairments.

Keywords: EEG, source analysis, neural control, gait, independent component analysis

Introduction

Identifying neural mechanisms involved in loss of balance during human walking could help in designing and targeting fall prevention interventions. Falls are a major problem in the elderly and many neurological patient populations (National Center for Injury Prevention and Control 2006). Injuries resulting from a fall can have a significant impact on an individual's ability to independently perform activities of daily living. Often the exact cause, timing or symptoms of a fall are not clear. Consequently, developing methods for fall prevention is challenging. Recent reviews have concluded that no single approach to fall prevention seems to work on the majority of the population at risk of falls (Chase et al. 2012; National Center for Injury Prevention and Control 2008; Shubert 2011). If specific neural mechanisms were identified as related to a specific fall cause or to individual subjects, it might be possible to better target a fall prevention/intervention method for a given patient.

Control of balance requires communication and integration across the nervous system. Preventing and recovering from loss of balance requires an integration of visual, vestibular, proprioceptive, and other sensory feedback mechanisms (Faraldo-Garcia et al. 2012; Sozzi et al. 2012). Standing posture has a clear feedforward component, as well as a dependence on sensory feedback (Lakie and Loram 2006; Loram et al. 2009). These and other studies (Ahmed and Ashton-Miller 2007; Merfeld et al. 1999) suggest that humans use an internal model of their body mechanics to sense and predict loss of balance. In addition, there are non-functional (short-latency) and 'feet-in-place' (medium-latency) postural adjustments that are controlled through spinal reflex and brainstem circuits (Adkin et al. 2006; Brown et al. 1999; Deliagina et al. 2012; Diener et al. 1985; Jacobs and Horak 2007; Loram and Lakie 2002; Rankin et al. 2000). Cortical areas activate long-latency movements that produce a change in base of support, such as stepping. Specifically, a cerebellar-cortical loop has been implemented in integrating prior experience into postural responses, and a basal ganglia-cortical loop is responsible for incorporating sensory information on the current posture (Jacobs and Horak 2007). There have been some imaging studies that have attempted to provide insight into the cortical mechanisms involved in whole body postural responses (Jacobs et al. 2008; Mochizuki et al. 2008, 2009a,b; Slobounov et al. 2000, 2005, 2006, 2008, 2009), but they have not explored human locomotion and the technical challenges that come with walking.

Recent technological advancements enable researchers to study electrocortical dynamics directly at the level of cortical sources, even during whole body movements including head motion (Gramann et al. 2011; Makeig et al. 2009). High-density electroencephalography (EEG) can be combined with independent component analysis (ICA) to identify electrocortical areas that are synchronized with the gait cycle during human walking (Gwin et al. 2011; Wagner et al. 2012). Studies that have used electroencephalography in other motor tasks, such as joystick

manipulation and standing postural perturbations, have identified that the anterior cingulate cortex is highly involved in error detection during motor tasks (Anguera et al. 2009; Gwin et al. 2011; Mochizuki et al. 2009a). In one recent study, Slobounov et al. (Slobounov et al. 2009) found significantly higher spectral power in low theta (4-5 Hz) and alpha (8-12 Hz) frequency bands from scalp electrodes located over the anterior cingulate during unstable balance when standing on one leg.

The purpose of this study was to identify specific cortical regions with spectral power modulations related to loss of balance during walking. We had healthy young subjects walk on a 2.5 cm wide by 2.5 cm tall treadmill-mounted balance beam (treadmill and motor learning studies described in Domingo et al. 2009, 2010) to induce experimental loss of balance during gait. We recorded high-density electroencephalography, electromyography, and body motion analysis to identify electrocortical and kinematic correlates of loss of balance. We hypothesized that the anterior cingulate and sensorimotor cortical areas would exhibit significant changes in spectral power in the theta frequency band related to loss of balance. We based this hypothesis on previous studies demonstrating increased spectral power from electroencephalography electrodes located near anterior cingulate and sensorimotor regions during motor errors (Anguera et al. 2009; Mochizuki et al. 2009b; Slobounov et al. 2009). Although past research has identified increased theta power in scalp EEG electrodes over these cortical regions of interest, that research has been on sitting/standing posture or hand/arm movement, not locomotion. During human locomotion, there is strong involvement of spinal locomotor networks and inhibition of cortical multisensory areas (Jahn and Zwergal 2010). As a result, it is not clear if results from standing whole body motor tasks can directly transfer to walking.

Another novel aspect of our study was the combination of high-density electroencephalography and electrocortical source imaging via independent component analysis and inverse head modeling. These techniques allowed us to look at specific cortical regions rather than relying on electrode locations for source localization. Our approach separated electrode channel signals into maximally independent source signals, factored out eye, muscle, and movement artifacts from brain electrical activity (Jung et al. 2000; Makeig et al. 1996; Onton and Makeig 2006) and then further identified distinct three-dimensional cortical source regions related to walking balance.

Methods

Subjects. Twenty-six healthy volunteers with no history of major lower limb injury and no known neurological or locomotor deficits completed this study. All subjects characterized themselves as right hand and right foot dominant (12 females and 14 males, 23 ± 5 years old (mean ± s.d.)). All subjects provided written informed consent. The University of Michigan Institutional Review Board approved the protocol and the study complied with the standards defined in the Declaration of Helsinki.

Data Collections. We mounted a 2.5 cm wide by 2.5 cm tall balance beam to the belt of a modified treadmill (Full Vision, Inc., Newton, KS). The balance beam consisted of small wooden blocks that lined up to make a continuous balance beam. We refer to this apparatus, which has been used in prior studies (Domingo and Ferris 2010; 2009), as a balance-beam treadmill (Figure 1).

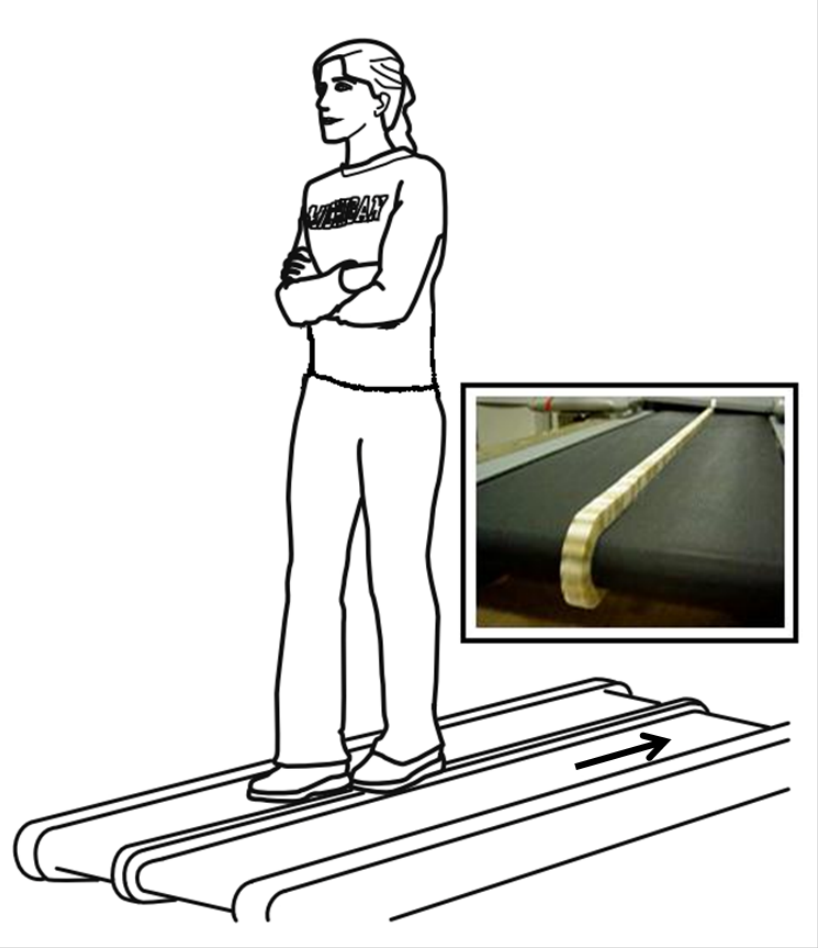

Fig. 1. A sketch of the experimental setup showing a subject walking on a treadmill mounted balance-beam. A picture of the balance-beam treadmill is also shown (inset).

Subjects performed *off-beam* and *on-beam* walking for 25 minutes each. Subjects took breaks as desired and no subject reported problems with fatigue. The total length of data collections varied from 60 minutes to 120 minutes due to subject breaks and technical requirements of the protocol. During off-beam walking subjects placed their feet on the treadmill belt on either side of the narrow balance beam. During on-beam walking subjects walked heel-to-toe (i.e., tandem). Subjects were instructed to maintain balance only by moving their torso and pelvis side-to-side (i.e., in the frontal plane). During both walking conditions subjects crossed their arms in front of their torso (Figure 1) and were instructed to look straight ahead at a flat white surface mounted in front of the treadmill. This controlled movement reduced variability otherwise arising from extraneous arm movement and thus enabled more reliable evaluation of motion and balance characteristics across subjects and trials. When subjects lost their balance (i.e., when they had to step off of the balance beam) they then were asked to perform 5 seconds of off-beam walking before attempting to re-mount the balance-beam. All subjects wore standardized orthopedic shoes. The treadmill belt speed was set at 0.22 m/s based on prior work in our lab (Domingo and Ferris 2010; 2009).

During both walking conditions we recorded motion, electromyography and electroencephalography data. We recorded the positions of 28 reflective markers using a motion capture system (Motion Analysis Corporation, Santa Rosa, CA, USA at 128 Hz or Vicon, Los Angeles, CA, USA at 100 Hz). We placed these markers on subjects' feet, legs, pelvis, neck and shoulders. To record lower limb electromyography (Konigsberg Instruments Inc., Pasadena, CA, USA at 1200 Hz or Biometrics Ltd., Ladysmith, VA, USA at 1000 Hz), we placed electrodes on the tibialis anterior, soleus, medial gastrocnemius and lateral gastrocnemius. We prepared the skin at each electrode site by shaving and cleaning with rubbing alcohol. We used tape to secure each electrode over the muscle belly along the long axis. We also secured the electrode wires to the limbs using athletic foam wrap. We recorded electroencephalography using a 256-channel active electrode array (sampling rate 512 Hz; Active II, Biosemi, Netherlands). Before data collection, we measured electrode impedance and used electrode gel to ensure that the impedance was less than 20 kΩ for each channel. The recording bandpass filter was DC to 104 Hz. During data collection, we positioned the electroencephalography amplifier above the subject and constrained wire movement to minimize motion artifact. Electrode impedance was monitored during subject collections and electrodes were re-gelled as needed to maintain an impedance of less than 20 kΩ for each channel.

Data Pre-processing. We identified gait events of heel strike and loss of balance from the motion data using Visual 3D software (C-Motion, Germantown, MD). A 6 Hz low-pass filter removed marker movement artifacts in motion capture data. We considered pelvic marker movement on/near the sacrum (S1/S2 vertebrae) to be representative of center of mass movement. Past

studies have found no significant differences between this approach and a more complicated body segment model at low walking speeds (Saini et al. 1998; Gard et al. 2004). We determined heel strike events for each foot (i.e., the times when the foot contacted the treadmill belt or balance beam) based on the velocity of a reflective marker on the ankle. Vertical ankle marker position was used to distinguish between foot contact with the treadmill belt (TC) and contact with the balance beam (BC).

We defined loss of balance as the subject stepping off the beam and onto the treadmill. In other words, loss of balance occurred between when a foot was in contact with the beam and the other foot contacted the treadmill belt. We did not identify an exact time that balance was lost as it could be defined at many times between the foot leaving the beam and making contact with the treadmill.

We performed all data analysis in Matlab (The Mathworks, Natick, MA, USA) using scripts based on EEGLAB, an open source environment for processing electrophysiological data (Delorme and Makeig 2004). We applied a second-order high-pass Butterworth filter with a 20 Hz cutoff frequency to the electromyography data to remove artifacts arising from electrode wire movement plus any DC offset. We then full-wave rectified the electromyography data. We synchronized the electroencephalography, electromyography, motion capture data, and gait events offline using a common analog timing signal. A 1 Hz high-pass filter removed drift in the electroencephalography data. We determined treadmill-contact (TC) and beam-contact (BC) events for each foot (i.e., the times when the foot contacted the treadmill belt or the balance-beam) based on the gait pattern of heel-strike and loss-of-balance events. Particularly noisy EEG channels were removed from the data. Initial channel rejection criteria were: a standard deviation larger than 1000 μV, kurtosis more than 3 standard deviations from the mean of all channels, or correlation coefficient with nearby channels less than 0.4. These criteria were adjusted for each subject's data to improve independent component analysis dipole localization and reduce residual variances between the independent component scalp maps and the computed scalp projections of the best-fitting single equivalent dipole component models. The remaining channels were average referenced. We retained 134±19 (mean ± s.d.) channels for each subject based on these criteria.

Analysis of Electrocortical Sources

For each subject, we used adaptive mixture independent component analysis (AMICA) (Delorme et al. 2012; Palmer et al. 2006; Palmer et al. 2008) to parse the electroencephalography signals into a sum of maximally independent component processes. Before performing independent component analysis decomposition, we concatenated electroencephalography data

from all experimental conditions for each subject to form a single data stream and removed periods of electroencephalography data with substantial artifact. We defined substantial artifact as z-transformed power across all channels in a given time window being larger than 0.8, but adjusted this value slightly for each subject's data to further improve our ability to localize the brain source components using a single dipole model (Delorme et al. 2012). The sizes of the data matrices so decomposed were 134 ± 19 channels (mean ± s.d.; min: 103; max: 168) by 944,890 ± 999,950 time points (mean ± s.d.; min: 799,880; max: 1,184,695) or 30.3 ± 3.3 minutes (mean ± s.d.; min: 26.0; max: 38.6) of data. This gave the decompositions a favorable mean ratio (time points to unmixing coefficients, here 134^2) of over 50, i.e., above our heuristic standard minimum of 30 based on results of previous analyses.

We fit a single equivalent current dipole model for each independent component using a boundary element method (BEM) head model based on the MNI brain (Montreal Neurological Institute, MNI, Quebec) as implemented in the EEGLAB DIPFIT toolbox (Oostenveld and Oostendorp 2002). We used component scalp maps learned by AMICA from the data as inputs for this modeling. We excluded independent components from further analysis when the equivalent current dipole was located outside of the cortical gray matter or when the projection of the (best-fitting) equivalent current dipole to the scalp (the dipole scalp map) accounted for less than 85% of the independent component scalp map variance. We also rejected independent components from further analysis if their topography, time course, and power spectrum were reflective of non-brain eye-movement or electromyographic processes (Jung et al. 2000a; Jung et al. 2000b). We assumed the remaining independent components (16 ± 8 per subject; min: 7; max: 46) reflected activity generated in a cortical source area close to the location of their equivalent dipole model (Akalin Acar and Makeig 2013).

Each time a subject stepped off the balance beam and onto the treadmill belt (i.e., lost their balance), we computed a single-trial time/frequency log spectrogram for each independent component source activity using 3-cycle Morlet wavelets. To enable averaging and statistical reliability testing, these spectrograms were linearly time-warped so that treadmill-contact and beam-contact events occurred at the same adjusted latencies in each spectrogram. The spectrograms were computed over a two-stride window (one stride before step-off and one stride after step-off). To visualize changes in the spectrograms associated with loss of balance, we subtracted the average log spectrum for the first step in the two-stride cycle from each latency of the mean event-related spectrogram (Makeig 1993). Time-warping of the spectrograms standardized the time intervals between five successive gait events, with the exact times defined based on the median values, rounded to the nearest 100 ms. Actual median event times for the time-warped gait events of beam contact (BC) and treadmill contact (TC) were 0, 1100, 2200,

3300, and 4400 ms (TC→TC→TC→TC→TC for steady-state balance beam trials; BC→BC→TC→TC→TC for loss of balance trials.

We analyzed trials of walking on and off the balance beam using the same methodology. We computed a single-trial time/frequency log spectrogram for each independent component source activity using 3-cycle Morlet wavelets. These spectrograms were linearly time-warped so that treadmill-contact events occurred at the same adjusted latencies in each spectrogram. Because walking on and off the balance beam are steady state tasks, the spectrograms were computed over a one-stride window. To visualize changes in the spectrograms associated with the gait cycle and steady state balance, we subtracted the average log spectrum for the entire stride cycle from each latency of the mean event-related spectrogram (Makeig 1993). Time-warping of the spectrograms standardized the time intervals between three successive gait events, with the exact times defined based on the median values, rounded to the nearest 100 ms. Actual median event times for the time-warped gait events of right treadmill contact (RTC) and left treadmill contact (LTC) were 1100, 2200, and 3300 ms (RTC→LTC→RTC). Time periods of 0 to 1100 ms and 3300 ms to 4400 ms were not included to enable evaluation of steady state walking (e.g. edge effects could exist in those time periods due to a subject about to lose balance or recovering from a loss of balance).

Group Analysis and Statistics. For group analysis, we clustered independent component sources from all subjects using EEGLAB routines implementing k-means clustering on vectors jointly coding differences in component equivalent dipole locations, scalp topographies (i.e., projection patterns of the independent component sourced to the scalp) and component mean log power spectra during on-beam and off-beam walking. Before clustering, the resulting joint vector was reduced to 10 principal dimensions using principal component analysis. Clusters containing components from fewer than 12 of the 26 subjects were excluded from further analysis.

We then computed grand mean log power spectra for on-beam and off-beam walking for each independent component cluster. For each cluster, we used Wilcoxon tests to evaluate mean power differences between conditions within a moving 2 Hz frequency window (α=0.05). Next, for each independent component cluster we created grand average baseline-normalized log spectrograms (Makeig 1993) for loss of balance events by averaging across data windows time locked to all loss of balance events for all subjects. Subjects who had fewer than three loss of balance events to either side (i.e., right foot step-off or left foot step-off) were not included in the loss of balance spectrograms (n=9). Altogether, the loss of balance analysis included a total of 302 trials from 17 subjects comprising 18±5 trials per subject (mean ± s.d.; min: 10 trials; max: 28 trials). Significant changes in spectral power during these trials, compared to baseline, were identified using the nonparametric bootstrapping statistical comparison approach in EEGLAB (α=0.05).

We created grand average baseline-normalized log spectrograms for each independent component cluster (Makeig 1993) for steady state walking on and off the balance beam by averaging across data windows time locked to treadmill-contact events for all subjects. Altogether, this steady state walking analysis included a total of 10,600 trials from 26 subjects comprising 204±110 trials per subject (mean ± s.d.; min: 28 trials; max: 623 trials). Significant changes in spectral power during these trials, compared to baseline, were identified using the nonparametric bootstrapping statistical comparison approach in EEGLAB (α=0.05).

Results

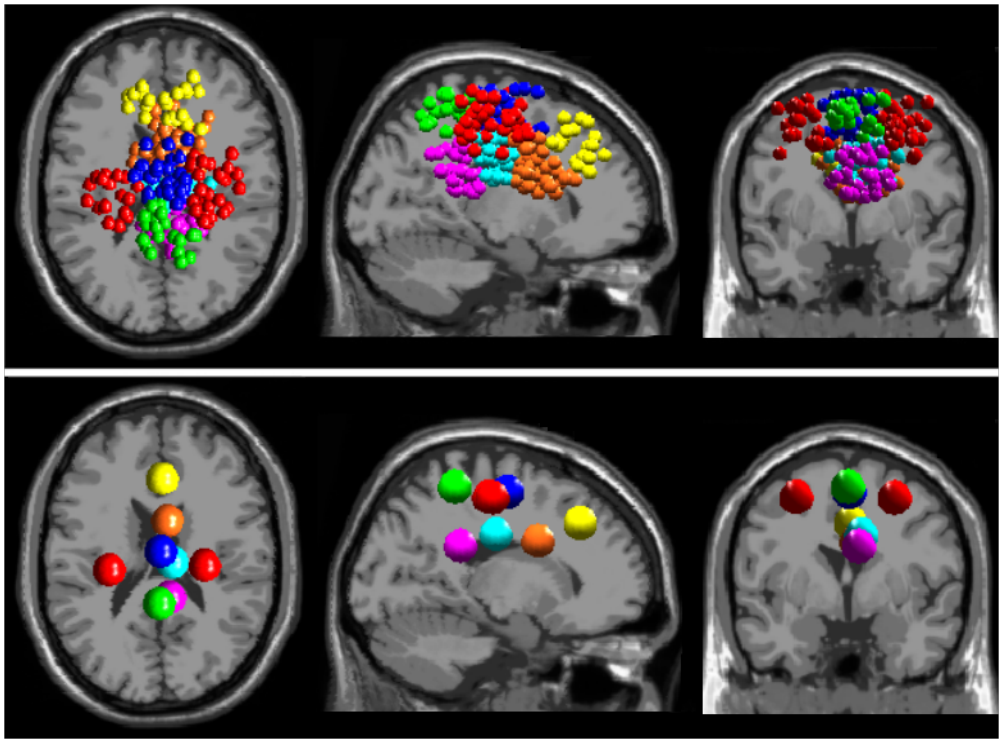

Fig. 2. Clusters of independent component (IC) EEG sources localized in and near anterior cingulate (orange), posterior cingulate (two clusters, magenta and cyan), superior dorsolateral prefrontal (yellow), anterior parietal (green), left and right lateral sensorimotor (red), and medial sensorimotor (blue) cortex. (Top row) small spheres indicate the equivalent current dipole locations of each clustered IC source. (Bottom row) larger spheres show the locations of the cluster centroids.

Independent component analysis produced clusters of electrocortical sources in or near anterior cingulate (52 sources, 21 subjects), posterior cingulate (two clusters; 40 sources, 16 subjects; 28 sources, 13 subjects), superior dorsolateral prefrontal (22 sources, 11 subjects), anterior parietal (22 sources, 12 subjects), left lateral sensorimotor (18 sources, 14 subjects),

right lateral sensorimotor (33 sources, 14 subjects), and medial sensorimotor (37 sources, 15 subjects) cortex (Figure 2).

It also identified clusters in or near insular cortex and visual cortex, but these clusters contained sources from 10 or fewer subjects. These clusters also had no areas of significant difference in their loss-of-balance spectrograms, nor significant changes in spectral power between on-beam versus off-beam walking. As a result, we excluded the insular and visual cortex clusters from further analysis.

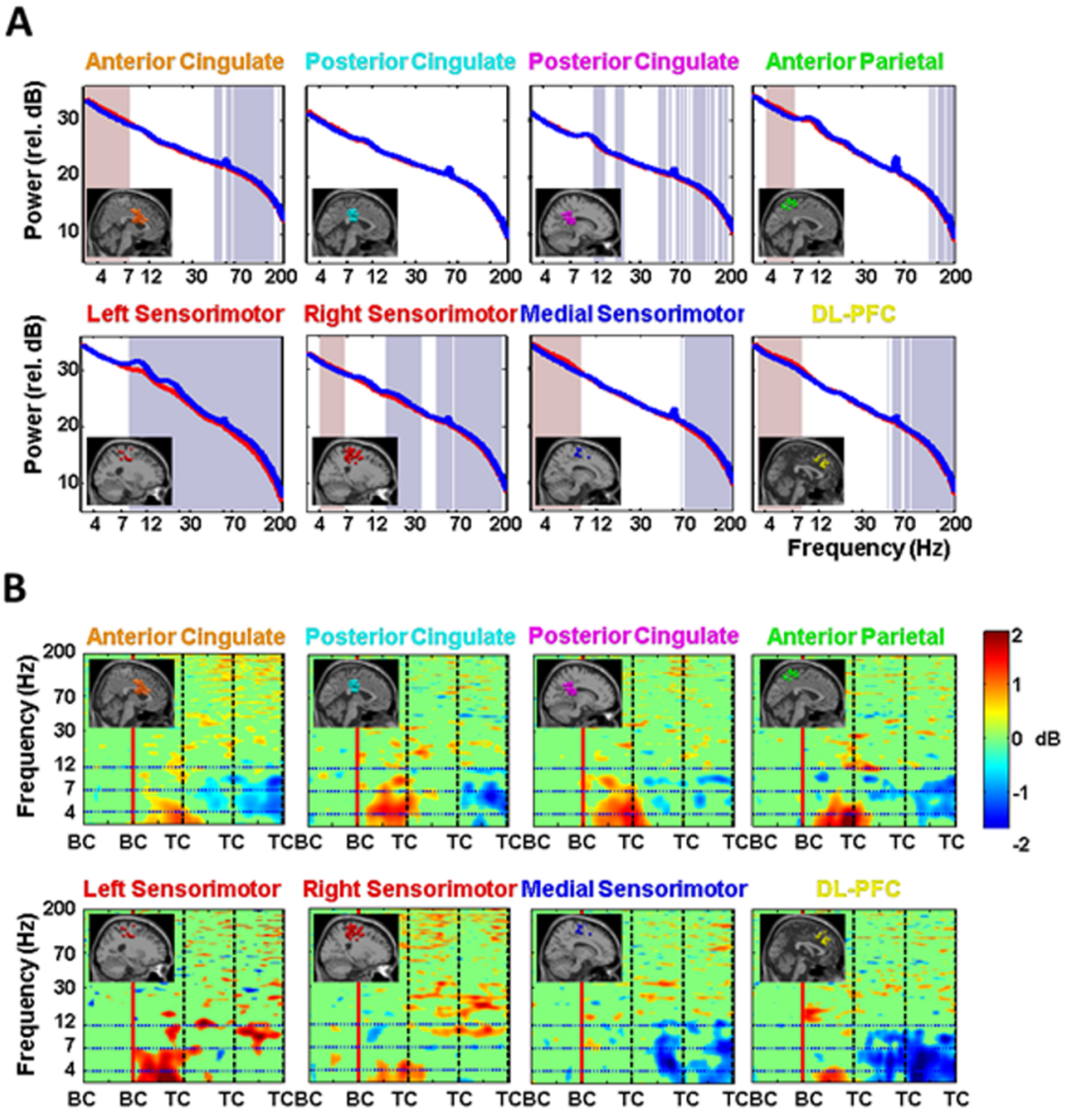

Fig. 3. A) Grand average spectral power for each cluster of electrocortical sources during walking on the balance beam (red line) and walking on the treadmill belt (off the balance beam)

(blue line). The lowest frequency shown is 3 Hz. Significant differences in spectral power between the on beam and off beam conditions are indicated by the shaded regions; reddish (theta band) regions indicate larger power in balance beam walking, bluish regions (higher frequencies) indicated larger power in treadmill walking ($p<0.05$). The colors of the plot titles correspond to the colors of the equivalent current dipoles in Figure 2. B) Grand average normalized log spectrograms showing changes in spectral power during and after loss of balance relative to average spectral power during the last successful step prior to loss of balance (left of the red vertical line). Mean step period (left BC to right BC) was 1100 ms. Four steps are shown, with BC indicating foot-to-Beam Contact and TC indicating foot-to-Treadmill Contact. After the second Beam Contact event, the subject loses balance and recovers by stepping off of the beam and onto the treadmill. Non-significant differences from baseline ($p>0.05$) have been set to 0 dB (green). The colors of the plot titles correspond to the colors of the equivalent current dipoles and dipole clusters in Figure 2. The left sensorimotor cluster plot averages only those trials where a loss of balance occurred toward the right side of the beam; the right sensorimotor cluster plot averages only those trials where a loss of balance occurred toward the left side of the beam. All other results shown here average all trials when a loss of balance occurred, both to the left and right. Theta spectral power increases began in the left sensorimotor sources, followed by the posterior cingulate, anterior cingulate and right sensorimotor sources, and finally in anterior parietal and superior dorsolateral-prefrontal sources.

During walking on the balance beam compared to walking on the treadmill belt, independent component sources in the left and right sensorimotor cortex clusters exhibited lower spectral power in the alpha (8-12 Hz) and beta (12-30 Hz) frequency bands, as well as in higher frequency bands (Figure 3A). This difference was significant for both hemispheres in the beta band, but was only significant for the alpha band in the left hemisphere cluster. Clustered independent component sources in or near anterior cingulate, anterior parietal, superior dorsolateral prefrontal, right sensorimotor and medial sensorimotor cortex exhibited significantly larger mean spectral power in the theta band (4-7 Hz) during walking on the balance beam compared to off-beam walking (Figure 3A).

Loss of balance analyses included 17 subjects with 18 ± 5 trials per subject (mean ± s.d.; min: 10 trials; max: 28 trials per subject), for a total of 302 trials. Data comprised 152 trials of electroencephalography, 148 trials of electromyography, and 157 trials of center of mass motion data for left side loss of balance, and 150 trials of electroencephalography, 149 trials of electromyography, and 156 trials of center of motion data for right side loss of balance. Missing data for some trials arose from movement artifacts and/or equipment malfunctions. Event times used for the time-warped gait events of beam contact (BC) and treadmill contact (TC) were 0,

1100, 2200, 3300, and 4400 ms (TC→TC→TC→TC→TC for steady state balance beam trials; BC→BC→TC→TC→TC for loss of balance trials).

All independent component source clusters except the medial sensorimotor cortex cluster exhibited a significant increase in theta band spectral power during loss of balance (i.e., before the first foot contact on the treadmill, TC, in these trials) (Figure 3B). The strongest power increase was in the left sensorimotor cortex cluster, which exhibited a 2 dB increase immediately at the beginning of double support with both feet on the balance beam (i.e., at the BC preceding TC in Figure 3B). Anterior cingulate, anterior parietal, superior dorsolateral prefrontal, and medial sensorimotor cortex exhibited alpha (8-12 Hz) and theta band (4-7 Hz) decreases in spectral power after first treadmill contact following loss of balance (Figure 3B).

For both loss of balance to the left and to the right, significant theta band increases in spectral power of left sensorimotor cluster sources occurred at the beginning of double support on the balance beam before losing balance (Figures 4 & 5). During losses of balance to the left side, in the right sensorimotor cluster there was generally a less pronounced and later change in theta band power. For losses of balance to the right side, there were no significant changes in theta band spectral power for the right sensorimotor cluster.

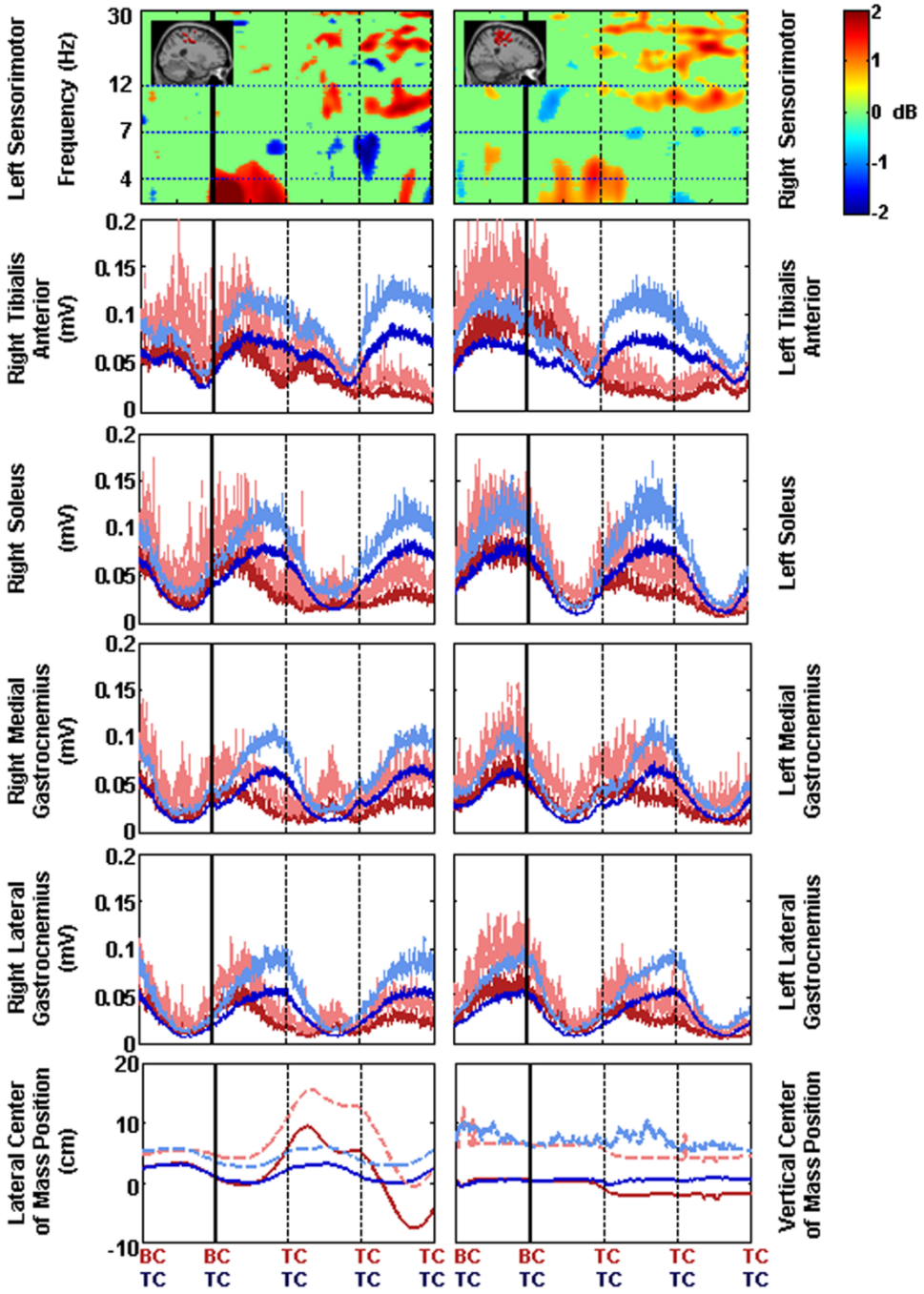

Fig. 4. Timing comparison of mean sensorimotor source cluster changes in EEG spectral power, lower leg EMG, and center of mass motion for losses of balance to the LEFT side of the beam. Four steps are shown (BC, beam contact; TC, treadmill contact). After the second BC (black vertical line), the subject loses balance and recovers by stepping off of the beam and onto the treadmill. For the sensorimotor cluster EEG spectral changes, non-significant differences from

baseline (p>0.05) have been set to 0 dB (green); the lowest frequency shown is 3 Hz. For the lower limb EMG and center of mass position data, red lines show loss of balance trial averages, blue lines are on beam walking averages, and dashed lines indicate +1 standard deviation. The cluster dipole images are replicated from Figure 3.

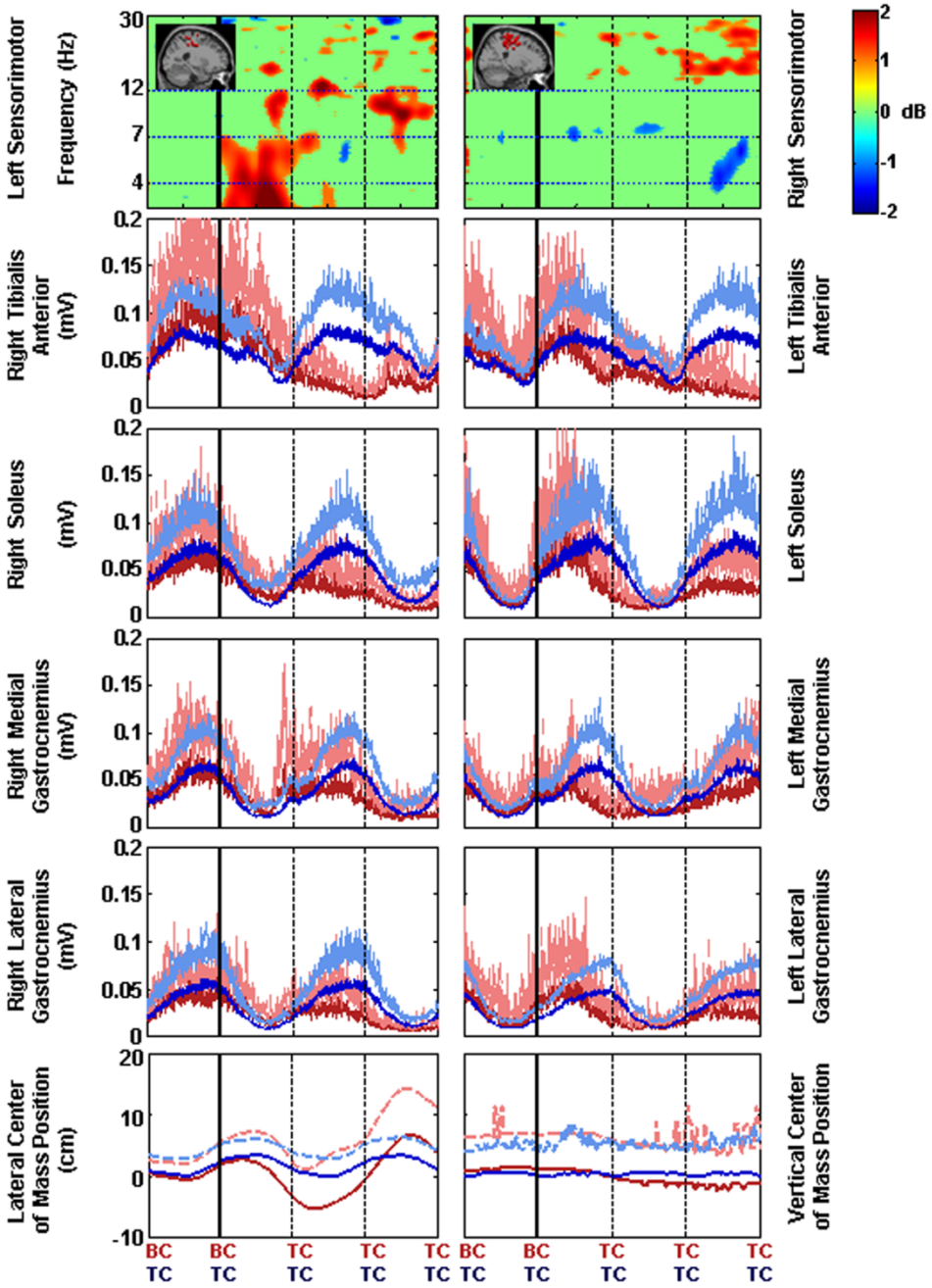

Fig. 5. Timing comparison of mean sensorimotor source cluster changes in EEG spectral power, lower leg EMG, and center of mass motion for losses of balance to the RIGHT side of the beam.

Four steps are shown (BC, beam contact; TC, treadmill contact). After the second BC (black vertical line), the subject loses balance and recovers by stepping off of the beam and onto the treadmill. For the sensorimotor cluster EEG spectral changes, non-significant differences from baseline ($p>0.05$) have been set to 0 dB (green); the lowest frequency shown is 3 Hz. For the lower limb EMG and center of mass position data, red lines show loss of balance trial averages, blue lines are on beam walking averages, and dashed lines indicate +1 standard deviation. The cluster dipole images are replicated from Figure 3.

Because the electromyography data for steady state beam walking were highly variable from step to step, the loss of balance muscle activity patterns in most cases did not diverge from steady state beam walking patterns beyond one standard deviation until after treadmill contact for the swing limb (Figures 4 & 5). The electromyography data for the stance or stabilizing limb (i.e. the limb that remained on the beam the longest) show loss of balance muscle activity patterns that diverge from steady state beam walking patterns beyond one standard deviation near the end of double support, i.e. the beginning of the swing phase in which the subject stepped off the beam. The large variations made electromyography data a poor predictor of when the loss of balance occurred. The lateral center of mass position data for the two conditions (loss of balance and steady state beam walking) show differences larger than one standard deviation at about the time of first treadmill contact after loss of balance (Figures 4 & 5). The vertical center of mass position data did not show any differences between the two conditions larger than one standard deviation.

Steady state walking on and off the beam electroencephalography analyses included 26 subjects with 204 ± 110 trials per subject (mean ± s.d.; min: 28 trials; max: 623 trials per subject), for a total of 10,600 trials. Event times used for the time-warped gait events of right treadmill contact (RTC) and left treadmill contact (LTC) were 1100, 2200, and 3300 ms (RTC→LTC→RTC). No independent component source clusters exhibited a significant increase in theta band (4-7 Hz) spectral power during steady state walking neither on nor off the balance beam (Figure 6). In fact, there are no sustained significant variations that appear to correlate with the gait cycle.

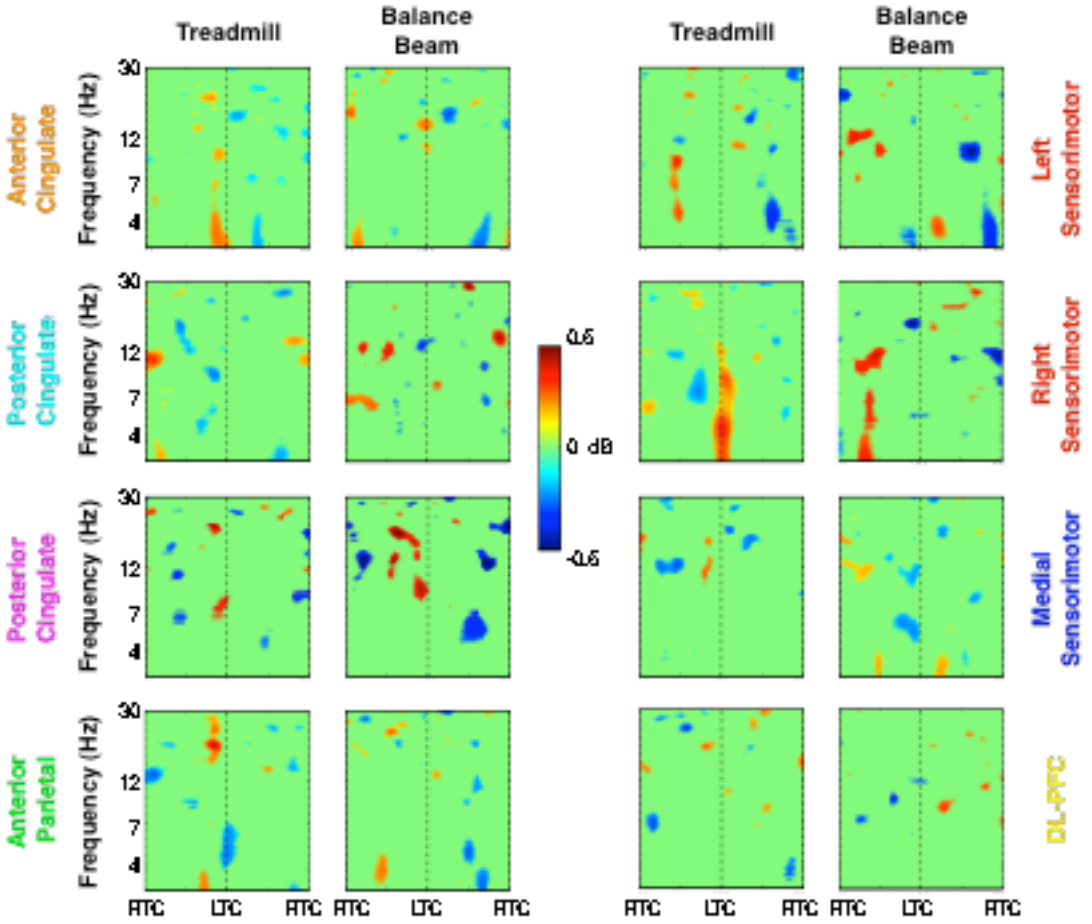

Fig. 6. Grand average normalized log spectrograms during walking off and on the balance beam (Treadmill and Balance Beam, respectively). Two steps are shown, with RTC indicating Right foot-to-Treadmill Contact and LTC indicating Left foot-to-Treadmill Contact. Mean step period was 1100 ms. Non-significant differences from baseline ($p>0.05$) have been set to 0 dB (green). The colors of the plot titles correspond to the colors of the equivalent current dipoles and dipole clusters in Figure 2. There were no substantial changes in theta spectral power during treadmill walking or balance beam walking compared to those seen during loss of balance on the balance beam (Figures 3-5).

Discussion

The purpose of this study was to assess electrocortical dynamics associated with maintaining and losing walking balance in humans. In particular, we hypothesized that anterior cingulate and sensorimotor cortical areas would exhibit significant theta band (4-7 Hz) electroencephalography power increases during loss of walking balance. When subjects lost their balance and stepped off

the narrow treadmill-mounted balance beam, significant increases in theta band spectral power occurred in independent component source clusters located in and near anterior cingulate, posterior cingulate, anterior parietal, left and right sensorimotor, and superior dorsolateral-prefrontal cortex. These spectral power increases arose at the beginning of double limb support with both feet on the balance beam. These changes in spectral power did not occur during steady state walking on or off the balance beam (Figure 6). This suggests that these broadly distributed electrocortical changes were specifically related to calculating an imminent loss of balance, and that sensory information from the leading limb contact with the balance beam was critical to the assessment of balance.

The first significant changes in electrocortical dynamics came from the left sensorimotor source cluster at the start of double support on the balance beam (Figure 3B). The theta band increase in right sensorimotor cortex was less pronounced than in the left sensoriomotor cortex (Figure 3B). This was true for both steps off to the right of the balance beam and steps off to the left of the balance beam (Figures 4 & 5). In fact, for steps off to the right, there were no significant changes in spectral power below 12 Hz during the loss of balance in the right sensorimotor source cluster. This suggests that, in these right-handed and -footed subjects, the left sensorimotor cortex plays a larger role in sensing loss of balance during walking than the right sensorimotor cortex. This conclusion is supported by previous literature indicating that the left hemisphere plays a more dominant role than the right hemisphere in skilled complex movements (Serrien et al. 2006). We note, however, that the medial sensorimotor region did not show significant theta activation associated with loss of balance.

Theta spectral power increases in other electrocortical regions also began during the double support phase, shortly after the theta spectral power increase in the left sensorimotor cortex (Figure 3B). Posterior cingulate and superior dorsolateral-prefrontal areas showed significant increases in theta spectral power, following similar increases in the left sensorimotor cluster but before those in anterior cingulate. Posterior cingulate cortex has been associated with self-referential processing, episodic memory, and vestibular functions (Kim 2012; Lopez et al. 2012). The involvement of this brain region in loss of balance is likely due to sensory/vestibular processing, and might provide information to the anterior cingulate, which exhibited a subsequent theta spectral power increase.

The superior dorsolateral prefrontal cortex cluster exhibited a theta spectral power increase similar to that of the anterior cingulate cluster. The source localization and scalp projections of the superior dorsolateral-prefrontal cluster suggests that theta spectral power from this cluster could be the neural generator largely responsible for scalp electrode signals attributed in other studies to ventral anterior cingulate, medial-frontal, frontocentral, or posterior

frontomedial cortices during error monitoring (Adkin et al. 2006; Debener et al. 2005; Dehaene et al. 1994; Luu et al. 2003; Maki and McIlroy 2007; Quant et al. 2004).

The increase in theta band power in the anterior cingulate cluster appears to have become significant somewhat after the theta band increases in posterior cingulate and superior dorsolateral-prefrontal clusters (Figure 3B). This supports the idea that a primary role of the anterior cingulate cortex in walking balance is in error detection. Past studies on human balance have speculated that the nervous system compares current sensory information with that expected from an internal forward-looking model, with sufficient mismatch triggering a postural response (Ahmed and Ashton-Miller 2005; 2004; 2007).

During loss of balance, both anterior parietal and anterior cingulate clusters exhibited significant concurrent increases in theta band power. The parietal lobe is involved in sensory information integration and generates decision-related activity (Romo and de Lafuente 2012). Information from the parietal lobe may contribute to anterior cingulate processing regarding error trend detection for walking balance.

Following loss of balance, upon adoption of a stable, off-beam gait both theta and alpha band spectral power decreased significantly below the stable beam-walking baseline (Figure 3B). This decrease was consistent across anterior cingulate, posterior cingulate, anterior parietal, medial sensorimotor and superior dorsolateral-prefrontal clusters.

In general, successful balance beam walking was associated with significantly higher mean theta band power in the anterior cingulate, anterior parietal, superior dorsolateral prefrontal, and right and medial sensorimotor cortical clusters compared to off-beam walking on the treadmill surface (Figure 3A). This is similar to findings for averaged scalp electrode data comparing unstable and stable single-leg standing postures (Slobounov et al. 2009). The higher theta band power did not show many significant changes within the gait cycle for either steady state walking on the balance beam or steady state walking off the balance beam (Figure 6). This suggests that walking involves baseline theta band activity (in regions shown in Figure 3A) that significantly increases with loss of balance (in regions shown in Figure 3B). Hence, what is commonly thought of as theta band error detection extends to postural error detection during gait and loss of balance during gait.

These findings show the earliest changes in left sensorimotor cortex activity occurred regardless of the direction of the loss of balance (to the left or right). The significant changes in left sensorimotor cortex activity occurred just as the subjects transitioned from single limb support to double limb support. The added proprioceptive information that comes from having both limbs on the balance beam compared to just one limb on the balance beam is likely crucial to computing and updating the sense of loss of balance. The second foot on the ground provides

proprioceptive information about center of mass calculations similar to how light touch with a finger can improve stability during standing or walking (Jeka 1997).

Because of the large step-to-step variability in the electromyography and center of mass position data, traditional metrics used for indicating deviations in these gait parameters (e.g., divergence by more than 1 standard deviation (Kao et al. 2010)) did not provide a clear indication of when loss of balance occurred. This result suggests that it is difficult to determine the moment that a person detects the loss of balance during gait from the muscle activation patterns and kinematics. Past studies have demonstrated that post hoc analysis of muscle activity and kinematics can discriminate between losses of balance and gait without loss of balance (Mak et al. 2011; Yang et al. 2011), but these analyses are not determining the time point that balance is lost in real time. Our data indicate that changes in the support limb electromyography amplitudes of more than 1 standard deviation may be useful in defining when corrective action for loss of balance begins but not when loss of balance is detected. In the future, it may be possible to use more portable, less obtrusive electroencephalography electrodes (Chi et al. 2012; Liao et al. 2011) to detect the exact moment humans detect their loss of balance during everyday activities.

A major limitation of our study was the difficulty in knowing the exact instant of biomechanical loss of balance. In many stance perturbation studies, researchers control for this limitation by controlling the timing of the external perturbation. For example, fixed-support (feet-in-place) postural control strategies during standing elicit activation of ankle muscles approximately 80-140 ms after perturbation (Maki and McIlroy 2007). In our study we did not apply discrete postural perturbations but instead, relied on naturally occurring loss of balance during a difficult walking balance task. However, this made it more difficult to discern the time marking the beginning of a loss of balance. The single trial loss of balance data showed wide variations in the timing of changes in cortical source power. The lack of an exact biomechanical loss of balance marker prevented us from calculating any loss of balance event related potentials (ERPs), which might be expected to include, e.g., an error-related negativity (ERN) (Luu et al. 2004). The analysis approach that we used included time-warping the single-trial spectrograms to intervals between ground contact events to allow event-locked averaging to multiple step events and statistical analysis of spectral power changes in cortical clusters (Figure 3B). Time-warping after translation of the single trials to spectrograms avoided frequency shifts that would have occurred if time-warping had been applied to the raw independent component data epochs.

Another limitation of our study concerned the treadmill walking control condition. We did not compare the beam walking to completely normal gait, but to a walking condition at a slower than normal speed with a slightly wider than normal step width (due to straddling the balance beam). The treadmill speed we used in all conditions, 0.22 m/s, was chosen to allow

subjects to successfully walk on the balance beam (Domingo and Ferris 2010; 2009). A typical walking speed for a healthy young subject is around 1.25 m/s. We did not want to introduce the confounding variable of walking speed into our comparison between treadmill and balance beam walking conditions. Relative to normal walking speeds, slow walking is less automatic from a neural perspective and less dependent on passive dynamics from a biomechanical perspective. As a result, slow walking may involve more cortical control than fast walking, making it infeasible to directly compare the results of this study to previous results using faster walking speeds (Gwin et al. 2011; 2010; Wagner et al. 2012).

One of the most important findings from our study was that several widely distributed cortical regions appear to be involved in sensing and detecting a loss of balance during walking. There was a significant mean increase in theta band spectral power for independent component electroencephalography sources localized to multiple cortical areas, including sensorimotor, anterior cingulate, and anterior parietal regions when our subjects experienced loss of balance on a narrow beam. This was not the case during steady state walking on the treadmill and steady state walking on the balance beam. This increase in theta band power in anterior cingulate cortex may likely be related to the posited function of the anterior cingulate cortex in error detection (Anguera et al. 2009; Gehring et al. 2012).

The observed spectral power increases in theta band source activity in several cortical areas were likely related to sensorimotor control, sensory information processing, and motor decision-making. The left sensorimotor cortex showed a stronger theta band response than the right sensorimotor cortex and appeared to precede the theta spectral power increase in anterior cingulate. The early appearance of increased theta spectral power beginning in the left sensorimotor cortex suggests the central nervous system recognized the loss of balance as soon as the both feet were on the balance beam for the last time.

The ensuing widespread theta band increases might reflect activity occurring across a cortical network to plan a corrective step and evaluate its possible biomechanical consequences with maximum precision. In summary, these results provide insight into the cortical brain dynamic substrates of human walking balance and suggest there is a multi-focal cortical network involved in detecting and correcting loss of walking balance.

Acknowledgments

The authors would like to thank Evelyn Anaka, Monica Majcher, Matt East, Sarah Weiss, Karen Bartling, Krista Marck, Sameer Singh, Jillian Lapinski, Chris Lesch and Ashley Stephenson for their assistance with subject data collection and biomechanical data processing.

Grants

This work was supported in part by the Office of Naval Research (N000140811215), Army Research Laboratory (W911NF-09-1-0139 & W911NF-10-2-0022), an Air Force Office of Scientific Research National Defense Science and Engineering Graduate Fellowship (32 CFR 168a), National Institutes of Health (R01 NS073649) and the University of Michigan Medical Rehabilitation Research Training Program funded by the National Institutes of Health (NIH), the National Institute of Child Health and Human Development (NICHD), the National Center for Medical Rehabilitation Research (NCMRR) (T32HD007422). The content is solely the responsibility of the authors and does not necessarily represent the official views of ONR, ARL, AFOSR, NICHD or NIH.

Disclosures

No conflicts of interest, financial or otherwise, are declared by the author(s).

Author Contributions

A.R.S., S.M., and D.P.F. contributed to the conception and design of the research; A.R.S. performed the experiments; A.R.S. and J.T.G. analyzed the data; A.R.S., J.T.G., S.M., and D.P.F. interpreted the results; A.R.S. and J.T.G. prepared the figures; A.R.S. and J.T.G. drafted the manuscript; A.R.S., J.T.G., S.M., and D.P.F. edited and revised the manuscript.

References

Adkin AL, Quant S, Maki BE, and McIlroy WE. Cortical responses associated with predictable and unpredictable compensatory balance reactions. *Exp Brain Res* 172: 85-93, 2006.
Ahmed AA, and Ashton-Miller JA. Effect of age on detecting a loss of balance in a seated whole-body balancing task. *Clin Biomech (Bristol, Avon)* 20: 767-775, 2005.
Ahmed AA, and Ashton-Miller JA. Is a "loss of balance" a control error signal anomaly? Evidence for three-sigma failure detection in young adults. *Gait Posture* 19: 252-262, 2004.
Ahmed AA, and Ashton-Miller JA. On use of a nominal internal model to detect a loss of balance in a maximal forward reach. *J Neurophysiol* 97: 2439-2447, 2007.
Akalin Acar Z, and Makeig S. Effects of Forward Model Errors on EEG Source Localization. *Brain Topogr* 2013.
Anguera JA, Seidler RD, and Gehring WJ. Changes in performance monitoring during sensorimotor adaptation. *J Neurophysiol* 102: 1868-1879, 2009.
Brown LA, Shumway-Cook A, and Woollacott MH. Attentional demands and postural recovery: the effects of aging. *J Gerontol A Biol Sci Med Sci* 54: M165-171, 1999.
Chase CA, Mann K, Wasek S, and Arbesman M. Systematic review of the effect of home modification and fall prevention programs on falls and the performance of community-dwelling older adults. *Am J Occup Ther* 66: 284-291, 2012.
Chi YM, Wang YT, Wang Y, Maier C, Jung TP, and Cauwenberghs G. Dry and noncontact EEG sensors for mobile brain-computer interfaces. *IEEE Trans Neural Syst Rehabil Eng* 20: 228-235, 2012.
Debener S, Ullsperger M, Siegel M, Fiehler K, von Cramon DY, and Engel A. Trial-by-trial coupling of concurrent electroencephalogram and functional magnetic resonance imaging identifies the dynamics of performance monitoring. *The journal of neuroscience* 25: 11730-11737, 2005.
Dehaene S, Posner M, and Tucker D. Localization of a neural system for error detection and compensation. *Psychol Sci* 5: 303–305, 1994.
Deliagina TG, Zelenin PV, and Orlovsky GN. Physiological and circuit mechanisms of postural control. *Curr Opin Neurobiol* 2012.
Delorme A, and Makeig S. EEGLAB: an open source toolbox for analysis of single-trial EEG dynamics including independent component analysis. *Journal of Neuroscience Methods* 134: 9-21, 2004.
Delorme A, Palmer J, Onton J, Oostenveld R, and Makeig S. Independent EEG sources are dipolar. *PLoS One* 7: e30135, 2012.
Diener HC, Ackermann H, Dichgans J, and Guschlbauer B. Medium- and long-latency responses to displacements of the ankle joint in patients with spinal and central lesions. *Electroencephalogr Clin Neurophysiol* 60: 407-416, 1985.
Domingo A, and Ferris DP. The effects of error augmentation on learning to walk on a narrow balance beam. *Exp Brain Res* 206: 359-370, 2010.
Domingo A, and Ferris DP. Effects of physical guidance on short-term learning of walking on a narrow beam. *Gait Posture* 30: 464-468, 2009.

Faraldo-Garcia A, Santos-Perez S, Crujeiras-Casais R, Labella-Caballero T, and Soto-Varela A. Influence of age and gender in the sensory analysis of balance control. *Eur Arch Otorhinolaryngol* 269: 673-677, 2012.

Gehring W, Liu Y, Orr J, and Carp J. The Error-Related Negativity (ERN/Ne). In: *The Oxford Handbook of Event-Related Potential Components*, edited by Luck S, and Kappenman E. New York: Oxford University Press, 2012, p. 231-294.

Gramann K, Gwin JT, Ferris DP, Oie K, Jung TP, Lin CT, Liao LD, and Makeig S. Cognition in action: imaging brain/body dynamics in mobile humans. *Rev Neurosci* 22: 593-608, 2011.

Gwin JT, Gramann K, Makeig S, and Ferris DP. Electrocortical activity is coupled to gait cycle phase during treadmill walking. *Neuroimage* 54: 1289-1296, 2011.

Gwin JT, Gramann K, Makeig S, and Ferris DP. Removal of movement artifact from high-density EEG recorded during walking and running. *J Neurophysiol* 103: 3526-3534, 2010.

Jacobs JV, and Horak FB. Cortical control of postural responses. *Journal of Neural Transmission* 114: 1339-1348, 2007.

Jeka JJ. Light touch contact as a balance aid. *Phys Ther* 77: 476-487, 1997.

Jung TP, Makeig S, Humphries C, Lee TW, McKeown MJ, Iragui V, and Sejnowski TJ. Removing electroencephalographic artifacts by blind source separation. *Psychophysiology* 37: 163-178, 2000a.

Jung TP, Makeig S, Westerfield M, Townsend J, Courchesne E, and Sejnowski TJ. Removal of eye activity artifacts from visual event-related potentials in normal and clinical subjects. *Clin Neurophysiol* 111: 1745-1758, 2000b.

Kao PC, Lewis CL, and Ferris DP. Joint kinetic response during unexpectedly reduced plantar flexor torque provided by a robotic ankle exoskeleton during walking. *J Biomech* 43: 1401-1407, 2010.

Kim H. A dual-subsystem model of the brain's default network: Self-referential processing, memory retrieval processes and autobiographical memory retrieval. *Neuroimage* 2012.

Lakie M, and Loram ID. Manually controlled human balancing using visual, vestibular and proprioceptive senses involves a common, low frequency neural process. *J Physiol* 577: 403-416, 2006.

Liao LD, Wang IJ, Chen SF, Chang JY, and Lin CT. Design, fabrication and experimental validation of a novel dry-contact sensor for measuring electroencephalography signals without skin preparation. *Sensors (Basel)* 11: 5819-5834, 2011.

Lopez C, Blanke O, and Mast FW. The human vestibular cortex revealed by coordinate-based activation likelihood estimation meta-analysis. *Neuroscience* 2012.

Loram ID, and Lakie M. Human balancing of an inverted pendulum: position control by small, ballistic-like, throw and catch movements. *J Physiol* 540: 1111-1124, 2002.

Loram ID, Lakie M, and Gawthrop PJ. Visual control of stable and unstable loads: what is the feedback delay and extent of linear time-invariant control? *J Physiol* 587: 1343-1365, 2009.

Luu P, Tucker DM, Derryberry D, Reed M, and Poulsen C. Electrophysiological responses to errors and feedback in the process of action regulation. *Psychol Sci* 14: 47-53, 2003.

Luu P, Tucker DM, and Makeig S. Frontal midline theta and the error-related negativity: neurophysiological mechanisms of action regulation. *Clin Neurophysiol* 115: 1821-1835, 2004.

Mak MK, Yang F, and Pai YC. Limb collapse, rather than instability, causes failure in sit-to-stand performance among patients with parkinson disease. *Phys Ther* 91: 381-391, 2011.
Makeig S. Auditory event-related dynamics of the EEG spectrum and effects of exposure to tones. *Electroencephalogr Clin Neurophysiol* 86: 283-293, 1993.
Makeig S, Gramann K, Jung TP, Sejnowski TJ, and Poizner H. Linking brain, mind and behavior. *International Journal of Psychophysiology* 73: 95-100, 2009.
Maki BE, and McIlroy WE. Cognitive demands and cortical control of human balance-recovery reactions. *Journal of Neural Transmission* 114: 1279-1296, 2007.
Merfeld DM, Zupan L, and Peterka RJ. Humans use internal models to estimate gravity and linear acceleration. *Nature* 398: 615-618, 1999.
Mochizuki G, Sibley KM, Cheung HJ, Camilleri JM, and McIlroy WE. Generalizability of perturbation-evoked cortical potentials: Independence from sensory, motor and overall postural state. *Neurosci Lett* 451: 40-44, 2009a.
Mochizuki G, Sibley KM, Cheung HJ, and McIlroy WE. Cortical activity prior to predictable postural instability: is there a difference between self-initiated and externally-initiated perturbations? *Brain Res* 1279: 29-36, 2009b.
National Center for Injury Prevention and Control C. *CDC Injury Fact Book*. Atlanta: Centers for Disease Control and Prevention;, 2006.
National Center for Injury Prevention and Control C. *Preventing Falls: How to Develop Community-based Fall Prevention Programs for Older Adults*. Atlanta: Centers for Disease Control and Prevention;, 2008.
Oostenveld R, and Oostendorp TF. Validating the boundary element method for forward and inverse EEG computations in the presence of a hole in the skull. *Human Brain Mapping* 17: 179-192, 2002.
Palmer JA, Kreutz-Delgado K, and Makeig S. Super-Gaussian Mixture Source Model for ICA. In: *Lecture Notes in Computer Science*, edited by Rosca J, Erdogmus D, Principe JC, and Haykin S. Berlin: Springer, 2006, p. 854-861.
Palmer JA, Makeig S, Kreutz-Delgado K, and Rao BD. Newton method for the ICA mixture model. In: *33rd IEEE International Conference on Acoustics and Signal Processing*2008, p. 1805-1808.
Quant S, Adkin AL, Staines WR, and McIlroy WE. Cortical activation following a balance disturbance. *Exp Brain Res* 155: 393-400, 2004.
Rankin JK, Woollacott MH, Shumway-Cook A, and Brown LA. Cognitive influence on postural stability: a neuromuscular analysis in young and older adults. *J Gerontol A Biol Sci Med Sci* 55: M112-119, 2000.
Romo R, and de Lafuente V. Conversion of sensory signals into perceptual decisions. *Prog Neurobiol* 2012.
Serrien DJ, Ivry RB, and Swinnen SP. Dynamics of hemispheric specialization and integration in the context of motor control. *Nat Rev Neurosci* 7: 160-166, 2006.
Shubert TE. Evidence-based exercise prescription for balance and falls prevention: a current review of the literature. *J Geriatr Phys Ther* 34: 100-108, 2011.
Slobounov S, Cao C, Jaiswal N, and Newell KM. Neural basis of postural instability identified by VTC and EEG. *Exp Brain Res* 199: 1-16, 2009.

Sozzi S, Do MC, Monti A, and Schieppati M. Sensorimotor integration during stance: Processing time of active or passive addition or withdrawal of visual or haptic information. *Neuroscience* 2012.
Wagner J, Solis-Escalante T, Grieshofer P, Neuper C, Muller-Putz G, and Scherer R. Level of participation in robotic-assisted treadmill walking modulates midline sensorimotor EEG rhythms in able-bodied subjects. *Neuroimage* 63: 1203-1211, 2012.
Yang F, Bhatt T, and Pai YC. Limits of recovery against slip-induced falls while walking. *J Biomech* 44: 2607-2613, 2011.